

BEHAVIOUR OF COMPOSITE PLATE GIRDERS WITH PARTIAL INTERACTION

Md Y. YATIM, Nandivaram E. SHANMUGAM, Wan BADARUZZAMAN

Department of Civil and Structural Engineering, Universiti Kebangsaan Malaysia, 43600 UKM Bangi, Selangor, Malaysia

Received 20 Dec 2011; accepted 8 Feb 2012

Abstract. This paper is concerned with the behaviour and strength of composite plate girders in which, the interaction between the steel plate girder and concrete slab is partial. Based on curvature compatibility principle, an approximate method is proposed from which, the shear capacity and deflection at any given load may be determined. The tension field action developed in web panels at the post-buckling stage is incorporated in the solutions. From the results obtained by using the proposed method, it is found that the flexural stiffness and failure load drop with decrease in degree of interaction. Comparisons are made between the results obtained through the proposed method and the corresponding ones from finite element analysis. A satisfactory correlation between the results in terms of behaviour and strength establishes the accuracy of the proposed method.

Keywords: composite plate girders, partial interaction, ultimate load, flexural behaviour, finite element method.

Reference to this paper should be made as follows: Yatim, M. Y. M.; Shanmugam, N. E.; Wan Badaruzzaman, W. H. 2013. Behaviour of composite plate girders with partial interaction, *Journal of Civil Engineering and Management* 19(Supplement 1): S1–S13. <http://dx.doi.org/10.3846/13923730.2013.801898>.

Introduction

Steel–concrete composite plate girders display greater strength and stiffness compared to the corresponding bare steel plate girder acting alone. This can be attributed to the contribution by concrete slab which, when added to the post-buckling strength of the thin webs results in larger shear strength (Baskar *et al.* 2002). Composite action is achieved when the concrete slab is firmly fixed to the top flange of the steel girder by mechanical forms of shear connection. The performance of composite girders is governed by the effectiveness of interaction between the interconnected elements. The possible loss in shear connection stiffness is mainly due to the deformation of shear connectors which permits relative slip at steel–concrete interface (Nie, Cai 2003; Queiroz *et al.* 2007). The behaviour of composite members depends on the type of shear connection between the two materials. Rigid shear connectors usually develop full composite action between the individual materials, thus the conventional principle of analysis of full interaction can be applied. In contrast, flexible shear connectors permit development of partial composite action due to strain incompatibility at the interface and therefore, the analysis procedures require consideration of the interlayer slip between the materials. Horizontal shear force exerted at the interface is

transferred from one element to another through the deformable connectors.

Owing to the complex mathematical problems in partial interaction theory (Johnson 2004), composite design is simplified by assuming perfect interaction between steel and concrete elements. In fact, the presence of slip induces significant additional curvature where ignorance of this effect may result in inaccurate predictions of load carrying capacity and deflection of composite girders. The flexible nature of shear connectors indicates that imperfect interaction always exists even in full composite design and reduced levels of shear connection results in increase of available rotations in the joint region of a continuous beam (Oehlers *et al.* 1997; Uy, Nethercot 2005). Moreover, the need for partial interaction design is essential when the top flange of girder cannot accommodate the number of shear connectors required for full interaction.

A considerable amount of research has been directed in the past towards the study of composite plate girders. Allison *et al.* (1982) tested composite plate girders subjected to combined bending and shear. A procedure to determine the shear strength was developed in accordance with the Cardiff tension field method (Porter *et al.* 1975; Evans *et al.* 1978). Small-scale thin webbed composite girders with diagonal stiffeners at end panels

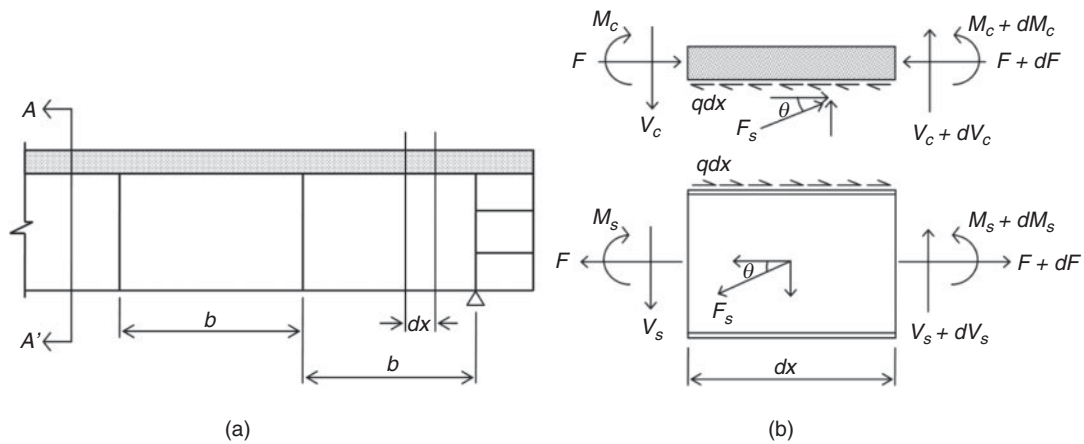


Fig. 1. Calculation model for a typical composite girder

were tested to failure by Porter and Cherif (1987). Methods for predicting shear strength of such girders are also presented. Shanmugam and Baskar (2003) carried out tests on composite plate girders to investigate the shear strength and concluded that the tension band width in webs increased due to composite action. A number of composite girders subjected to negative bending were also tested to failure (Baskar, Shanmugam 2003).

Second-order differential equation allowing for slip in composite beams was first developed by Newmark *et al.* (1951) by assuming equal curvature between the interacting elements. Experimental studies were conducted on composite beams subjected to single concentrated load applied at the mid-span. Expressions for slip and deflection were derived accounting for imperfect interaction. Adekola (1968) presented an interaction theory for composite beams allowing for interface friction, slip and uplift deformation. Fourth- and second-order coupled differential equations were derived and solved by finite difference method. It was found that the uplift deformation is insignificant. Further works on partial interaction in simply supported composite beams (Bradford, Gilbert 1992; Xu, Wu 2007) and continuous ones (Seracino *et al.* 2004, 2006) have been reported in the past.

An approximate method is developed in this paper to determine the load–deflection relationships and to predict the ultimate strength of simply supported composite

plate girders with partial interaction. The girder may be subjected to concentrated loads or uniformly distributed load on the entire span. The degree of interaction is specified by varying the longitudinal spacing of shear connectors along the span. Nevertheless, the uplift deformation or separation between elements is negligible as it is assumed that, both elements deflect equally with the same amount of curvature along the length. The long-term effects such as creep and shrinkage in the concrete are also disregarded herein.

1. Analytical method

In a composite plate girder with transverse stiffeners spaced at a distance b along the span, consider a finite length, dx of the web panel near the support as shown in Figure 1(a). The normal force acting at steel–concrete interface may be disregarded since the uplift deformation is not taken into account in this study. Free body diagrams of the finite length of the web panel and the concrete slab are shown along with the internal forces in Figure 1(b).

In the above figures, M_c and M_s are, respectively, moment carried by concrete slab and steel girder, V_c and V_s are the corresponding shear forces, F is the compressive or tensile force exerted on concrete or steel, F_s is the tensile membrane forces in the web introduced in the post-buckling stage and q is the horizontal shear force at the

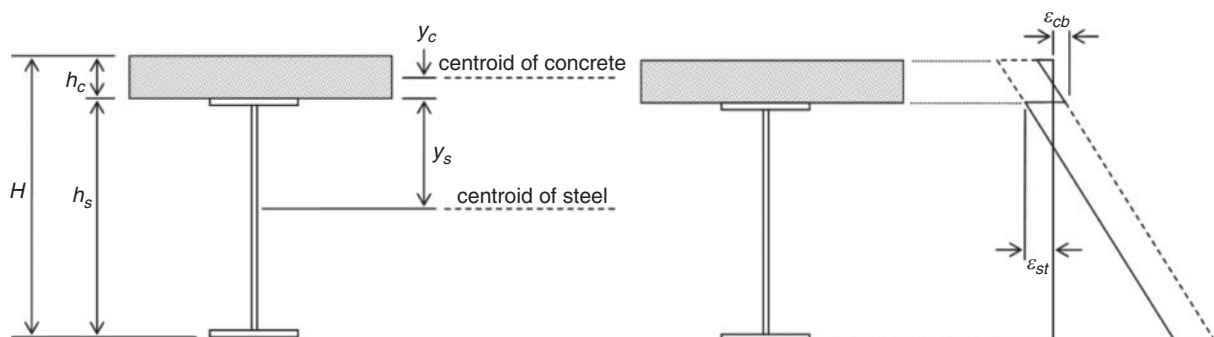


Fig. 2. Cross-section and strain distribution along the depth of a composite girder

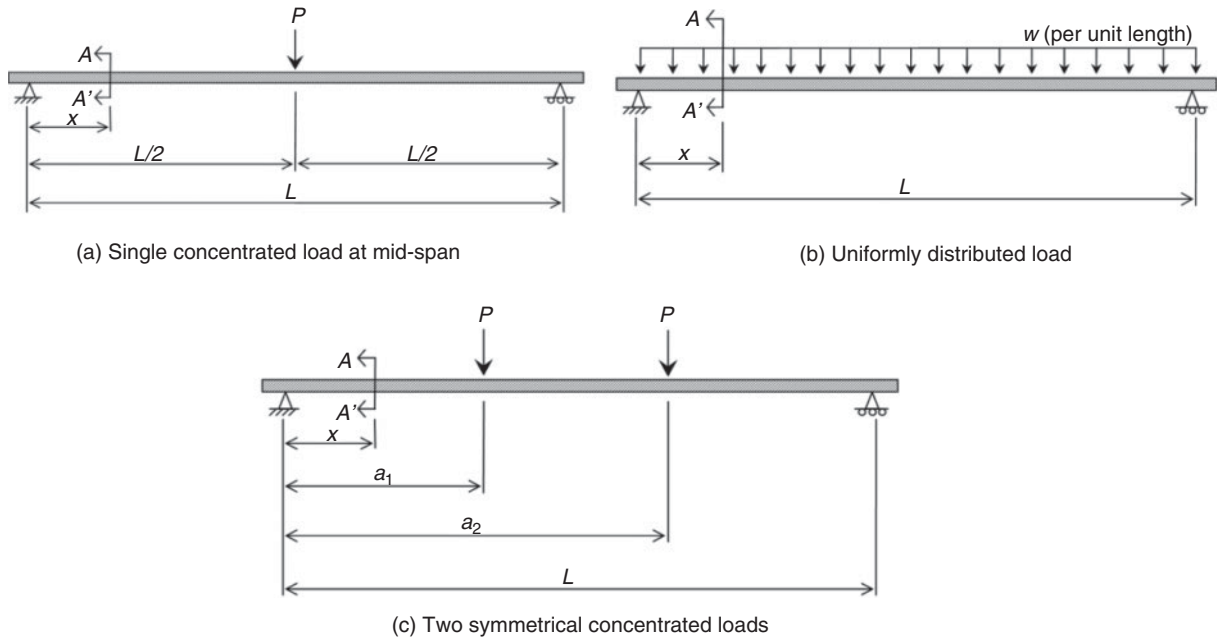


Fig. 3. Load definitions: (a) single concentrated load at mid-span; (b) uniformly distributed load; (c) two symmetrical concentrated loads

steel–concrete interface. The cross-section $A-A'$ of the composite girder along with the strain distribution across the depth is shown in Figure 2. Three different load conditions viz. single concentrated load applied at mid-span, uniformly distributed load along the entire span and symmetrically placed two concentrated loads, considered in the present study, are shown in Figure 3(a)–(c). In this figure, x refers to distance from the left support of any section $A-A'$ along the span.

1.1. Slip expressions

Equilibrium consideration of horizontal forces acting on concrete slab and steel girder in Figure 1(b) gives:

$$\frac{dF}{dx} = -q + \frac{F_s \cos \theta}{b}, \quad (1)$$

where θ is the angle of inclination of tensile membrane forces in the web panel. Assuming that the amount of slip, s , is directly proportional to q , one may write:

$$q = \frac{ks}{p}, \quad (2)$$

where k is shear stiffness of the connectors and p is the longitudinal pitch between connectors along the span length of the girder. Distribution of strain along the depth of concrete slab and steel girder is assumed to be linear as shown in Figure 2. Strain at the bottom of concrete slab, ϵ_{cb} , and that at the top of steel, ϵ_{st} , are given as:

$$\epsilon_{cb} = \frac{M_c y_c}{E_c I_c} - \frac{F}{E_c A_c}; \quad (3)$$

$$\epsilon_{st} = -\frac{M_s y_s}{E_s I_s} + \frac{F}{E_s A_s}, \quad (4)$$

where E_c , I_c and A_c are referred to as Young’s modulus, second moment of area and cross-section area of concrete, respectively, and E_s , I_s and A_s are the respective values for steel. The rate of change in slip along the steel–concrete interface (Nie, Cai 2003) may be calculated as:

$$\frac{ds}{dx} = \epsilon_{cb} - \epsilon_{st}. \quad (5)$$

Employing the curvature compatibility principle (Newmark *et al.* 1951), the curvature may be expressed as:

$$\frac{d^2 Y}{dx^2} = \frac{M_c}{E_c I_c} = \frac{M_s}{E_s I_s} = \frac{M - F d_c}{E_c I_c + E_s I_s}, \quad (6)$$

where Y is the total deflection of the entire section, M is the moment carried by the entire section and $d_c = y_c + y_s$. In view of Eqns (3), (4) and (6), the relative slip strain in Eqn (5) may be expressed as:

$$\frac{ds}{dx} = \alpha(M - F d_c) - \beta F \quad (7)$$

and

$$\frac{d^2 s}{dx^2} = \alpha \left[\frac{dM}{dx} - d_c \left(\frac{dF}{dx} \right) \right] - \beta \left(\frac{dF}{dx} \right), \quad (8)$$

where $\alpha = d_c / (E_c I_c + E_s I_s)$ and $\beta = (E_c A_c + E_s A_s) / E_c A_c E_s A_s$. For girders subjected to a single concentrated load as in Figure 3(a), the general expressions for moment at any section along the span are:

$$M_{pl1} = \frac{Px}{2} \quad \text{for } 0 \leq x \leq L/2; \quad (9)$$

$$M_{pl2} = \frac{P}{2}(L - x) \quad \text{for } x > L/2. \quad (10)$$

Substitution of Eqns (1), (2) and (9) into Eqn (8) yields:

$$\frac{d^2s}{dx^2} = \alpha \left[\frac{P}{2} - d_c \left(\frac{F_s \cos \theta}{b} - \frac{ks}{p} \right) \right] - \beta \left(\frac{F_s \cos \theta}{b} - \frac{ks}{p} \right). \quad (11)$$

Integrating Eqn (11) twice, with boundary conditions $ds/dx = 0$ at $x = 0$ and $s = 0$ at $x = L/2$, the slip expression may be simplified as:

$$s_1 = \frac{\alpha P - 2\psi \left(\frac{F_s \cos \theta}{b} \right)}{[16/(4x^2 - L^2)] - 2\psi K}, \quad \text{for } 0 \leq x \leq L/2. \quad (12)$$

Similarly, with Eqn (10) for moment and satisfying boundary conditions $ds/dx = 0$ at $x = L$ and $s = 0$ at $x = L/2$, slip solution for right-hand side of the applied load reduces to:

$$s_2 = \frac{\alpha P + 2\psi \left(\frac{F_s \cos \theta}{b} \right)}{(4/[(x - L/2)(3L/2 - x)]) + 2\psi K}, \quad \text{for } x > L/2, \quad (13)$$

where $\Psi = \alpha d_c + \beta$ and $K = k/p$.

As for uniformly distributed load case, similar procedures may be carried out using the respective moment expressions. Satisfying the boundary conditions $ds/dx = 0$ at $x = 0$ and L and $s = 0$ at $x = L/2$, the following slip expressions are obtained for $0 \leq x \leq L/2$ and $L/2 < x \leq L$, respectively:

$$s_1 = \frac{-\alpha w(L^3 - 6Lx^2 + 4x^3) + 3\psi(L^2 - 4x^2) \left(\frac{F_s \cos \theta}{b} \right)}{24 + 3\psi K(L^2 - 4x^2)}; \quad (14)$$

$$s_2 = \frac{-\alpha w(L^3 - 6Lx^2 + 4x^3) - 3\psi(3L^2 - 8Lx + 4x^2) \left(\frac{F_s \cos \theta}{b} \right)}{24 - 3\psi K(3L^2 - 8Lx + 4x^2)}. \quad (15)$$

For a girder subjected to two point loads of equal magnitude, P as shown in Figure 3(c), slip expressions may be derived with appropriate boundary conditions as:

$$s_1 = \frac{\alpha P(2L - a_1 - a_2) - \psi L \left(\frac{F_s \cos \theta}{b} \right)}{[2L/(x^2 - a_1^2)] - \psi LK}, \quad \text{for } 0 \leq x \leq a_1; \quad (16)$$

$$s_2 = \frac{\alpha p(a_1 + a_2) + \psi L \left(\frac{F_s \cos \theta}{b} \right)}{[2L/(a_2^2 - 2La_2 + 2Lx - x^2)] + \psi LK}, \quad \text{for } x \geq a_2. \quad (17)$$

1.2. Slip-induced deflection

The interlayer slip induces additional curvature when a composite girder bends. The slip-induced curvature may

be obtained from (Nie, Cai 2003):

$$\frac{d^2(\Delta y)}{dx^2} = \frac{1}{H} \left(\frac{ds}{dx} \right). \quad (18)$$

For the girder under single concentrated load, substituting the first derivative of Eqn (12) into Eqn (18) and performing double integration with boundary conditions $d(\Delta y)/dx = 0$ at $x = L/2$ and $\Delta y = 0$ at $x = 0$, the expression for slip-induced deflection, Δy can be obtained as:

$$\Delta y = \frac{1}{H\psi LKb\phi} \left[\frac{\alpha P b L}{2} - \psi L F_s \cos \theta \right] \times \left[2 \tanh^{-1} \left(\frac{\psi K x}{\phi} \right) + \phi x \right], \quad (19)$$

where $\phi = \sqrt{\left(\frac{8 + \psi K L^2}{4} \right) \psi K}$.

Similarly, the expressions for Δy derived using the appropriate boundary conditions for the girders subjected to uniformly distributed load or two concentrated loads may be given, respectively, as:

$$\Delta y = \frac{1}{H\psi K b \varpi^3} \left[\begin{aligned} & \left\{ 4\psi K \tanh^{-1} \left(\frac{2\psi K x}{\varpi} \right) \right\} \\ & \left\{ \alpha L b w \left(4 + \frac{2}{3} \psi L^2 K + \frac{1}{48} \psi^2 L^4 K^2 \right) - \psi F_s \cos \theta (\psi L^2 K + 8) \right\} + \\ & \left\{ \ln \left(\frac{\varpi^2}{\psi K} - 4\psi K x^2 \right) - \ln \left(\frac{\varpi^2}{\psi K} \right) \right\} + \\ & \left\{ \psi K x \varpi \left(\frac{\psi F_s \cos \theta (8 + \psi L^2 K) + 4\alpha w b \left[\frac{8L - \psi L^3 K}{8} + \frac{8x + \psi K x}{24} \right]}{4\alpha w b \left[\frac{8L - \psi L^3 K}{8} + \frac{8x + \psi K x}{24} \right]} \right) \right\} \end{aligned} \right], \quad (20)$$

where $\varpi = \sqrt{(8 + \psi K L^2) \psi K}$

and

$$\Delta y = \frac{1}{H\psi LKb\varphi} [\alpha P b(2L - a_1 - a_2) - \psi L F_s \cos \theta] \left[2 \tanh^{-1} \left(\frac{\psi K x}{\varphi} \right) - \varphi x \right], \quad (21)$$

where $\varphi = \sqrt{(2 + \psi K a_1^2) \psi K}$.

2. Strength parameters

2.1. Shear strength of concrete slab

One of the approximate methods to predict the strength of composite plate girders is by simply adding the shear strength of concrete slab to the shear capacity of steel girder acting alone (Narayanan et al. 1989). To account for partial shear connection, the following relationship is introduced assuming that the degree of interaction does not affect the shear strength of steel plate girder:

$$V_{cc} = V_a + \frac{N}{N_f} (V_f - V_a), \quad (22)$$

where V_{cc} is the shear resistance of the concrete slab in girders with partial interaction, V_a is the shear resistance of concrete slab alone (Eurocode 2 2004), V_f is the shear resistance of concrete slab for girders with full interaction, N is the actual number of shear connectors provided and N_f is the number of shear connectors required to achieve full shear connection (Johnson 2004). It should be noted that V_f is taken equal to the pull-out capacity of shear connectors (Liang *et al.* 2004). For full shear connection, i.e. $N/N_f = 1$, Eqn (22) reduces to $V_{cc} = V_f$.

Results from extensive finite element analyses on composite plate girders with different degrees of interaction showed that approximately 40% of the slab shear strength, denoted as $V_{cc,e}$, occurs within the elastic stage with remaining percentage, denoted as $V_{cc,pb}$, in the post-buckling phase. Thus, in the analysis presented herein, the contribution in the elastic and post-buckling phases, by the concrete slab to the shear capacity of the girders is assumed in the same proportion as that predicted by the finite element results.

2.2. Buckling load

At the elastic stage, critical shear strength, V_{cr} that causes buckling in the web plate is taken as the sum of web panel shear resistance and the strength contribution by concrete slab in the elastic phase, $V_{cc,e}$ i.e.:

$$V_{cr} = \tau_{cr}dt + V_{cc,e}, \quad (23)$$

where d is the depth of the web panel, t is the web panel thickness and τ_{cr} is the critical shear stress of web panel given as:

$$\tau_{cr} = C \left[\frac{\pi^2 E_s}{12(1-\nu^2)} \right] \left(\frac{t}{d} \right)^2, \quad (24)$$

where C is the buckling coefficient and ν is the Poisson's ratio of web material. For a simply supported girder subjected to concentrated load at mid-span, one can simply determine the load corresponding to buckling from:

$$\frac{P_{cr}}{2} = \tau_{cr}dt + V_{cc,e}. \quad (25)$$

From equilibrium, the shear carried by each of the supports of a composite girder at any load beyond elastic buckling may be expressed as:

$$V_C = V_{cr} + V_{cc,pb} + F_s \sin \theta, \quad (26)$$

where $V_{cc,pb}$ is shear strength contributed by the concrete slab beyond elastic buckling phase. In view of Eqn (23) and since $V_{cc} = V_{cc,e} + V_{cc,pb}$, Eqn (26) may be written as:

$$V_C = \tau_{cr}dt + V_{cc} + F_s \sin \theta. \quad (27)$$

For the simply supported girder with a concentrated load applied at the mid-span, the applied load, P may be computed from:

$$\frac{P}{2} = \tau_{cr}dt + V_{cc} + F_s \sin \theta. \quad (28)$$

2.3. Tension field force in the web panel

In accordance with the tension field theory, once the web plate has lost its capacity to sustain any further increase in compressive stress, a new load carrying mechanism is developed. Further loading beyond buckling is supported by an inclined tensile membrane field in the web. The resultant tensile force is given as:

$$F_s = \sigma_t b_{tf}, \quad (29)$$

where σ_t is the tensile membrane stress and b_{tf} is the width of diagonal tension band developed in the web panel determined in accordance with the Cardiff mechanism (Porter *et al.* 1975; Evans *et al.* 1978). Rearranging Eqn (28), an expression for F_s can be obtained as

$$F_s = \frac{P - 2(\tau_{cr}dt + V_{cc})}{2 \sin \theta}, \quad (30)$$

where when substituted in Eqn (29) yields σ_t as:

$$\sigma_t = \frac{P - 2(\tau_{cr}dt + V_{cc})}{2tb_{tf} \sin \theta}. \quad (31)$$

It should be noted that in the elastic stage, $F_s = 0$. Additionally, the applied load, P beyond elastic limit is sustained by the tensile membrane stress, σ_t in the web panel.

3. Load–deflection behaviour

3.1. Effective flexural stiffness

The bending stiffness of a composite section is significantly governed by the shear connection stiffness. Even in a composite design with full interaction, the interface shear transfer is not completely perfect and stiffness may be reduced to some extent due to flexibility of shear connectors. In this study, effective bending stiffness, EI_{eff} is employed in accordance with the principle suggested by Girhammar (2009). The flexural stiffness for composite section with perfect interaction may be written as:

$$EI_{\infty} = EI_0 + \frac{EA_p d_c^2}{EA_0}, \quad (32)$$

where EI_0 is the flexural stiffness of the section with no interaction, EA_p is the product of axial stiffness of the sub-elements and EA_0 is the sum of the axial stiffness of the sub-elements. To account for partial interaction, the effective bending stiffness is computed as:

$$EI_{eff} = EI_0 + \xi \left(\frac{EA_p d_c^2}{EA_0} \right), \quad (33)$$

where $\xi = \left[1 + \frac{\pi^2 EA_p}{KL^2 EA_0} \right]^{-1}$ for simple support conditions.

It should be noted that EI_{eff} remains constant throughout the elastic phase. Upon buckling, the rigidity changes proportional to the applied load. The EI_{eff} value at post-buckling state should, therefore, be computed at every load increment using tangent modulus, E_t (Timoshenko, Gere 1961) in place of constant E_s value

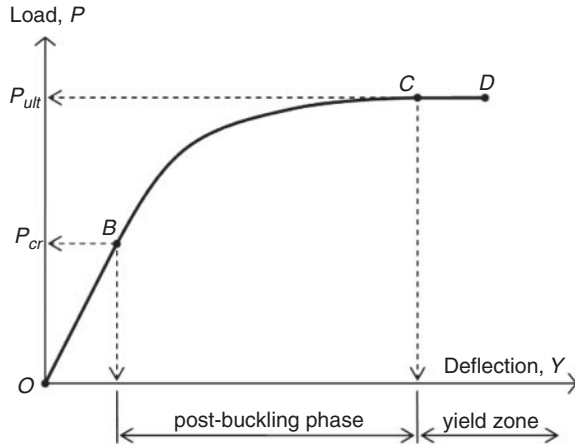


Fig. 4. Construction of load-deflection behaviour

in Eqn (32). Tangent modulus may be expressed as:

$$E_t = E_s \frac{\sigma_{yw} - \sigma_\theta}{\sigma_{yw} - \omega \sigma_\theta}, \quad (34)$$

where σ_{yw} is the yield stress of web material, ω is a constant and σ_θ is the resulting tensile stress given as:

$$\sigma_\theta = \tau_{cr} \sin 2\theta + \sigma_t. \quad (35)$$

3.2. Total deflection

Deflection of the whole composite section is computed at every load increment. The total deflection, Y is the sum of bending deflection, y_b , shear deflection, y_v and slip-induced deflection, Δy . For a girder under single point load applied at the mid-span, deflection at the elastic and post-buckling stages may be expressed, respectively, as:

$$Y_e = \frac{PL^3}{48(EI_{eff})_e} + \frac{PL(1+\nu)}{2E_s A_w} + \Delta y_e; \quad (36)$$

$$Y_{pb} = \frac{PL^3}{48(EI_{eff})_{pb}} + \frac{PL(1+\nu)}{2E_t A_w} + \Delta y_{pb}, \quad (37)$$

where Y_e , Δy_e and $(EI_{eff})_e$ refer to total deflection, slip-induced deflection and effective flexural stiffness, respectively, in the elastic stage, Y_{pb} , Δy_{pb} and $(EI_{eff})_{pb}$ are the respective values in the post-buckling stage, ν is the Poisson ratio and A_w is the shear area. The contribution by the concrete slab is ignored for shear deflection.

Substituting in Eqns (36) and (37), the relevant parameters for the composite plate girder subjected to a single concentrated load applied at the mid-span, load-deflection curve $OBCD$ can be plotted as shown in Figure 4. Point B refers to the upper limit of the elastic buckling stage given by Eqn (25). Beyond this stage, the load-deflection response exhibits different behaviour compared to the unbuckled state. The change in slope shown by curve BC is due to the reduced flexural rigidity calculated from Eqn (33) which induces larger deflection even for small increment in P when approaching the yield point. The girder reaches its capacity at the point C when the resulting stress, σ_θ obtained from Eqn (35) reaching the yield stress of the web panel, σ_{yw} . Further increase in deflection does not result in appreciable increase in applied load, P beyond this point. Thus, the load-deflection curve levelled off as shown by CD . Similarly, the load-deflection plots for other load conditions may be obtained. The ultimate load for the girder is obtained as the load corresponding to the peak point of the load-deflection plot.

4. Accuracy of the proposed method

Four composite plate girders namely CPG 1, CPG 2, CPG 7 and CPG 8 tested earlier by other researchers (Shanmugam, Baskar 2003; Baskar, Shanmugam 2003) were employed in the present study in order to establish the accuracy of the proposed method and to assess the influence of partial interaction. The relevant details of the girders are given in Table 1. These girders were originally tested under concentrated load applied at the mid-span. In the current study, all these girders were analysed by the proposed method and also by finite element modelling using the finite element package LUSAS. Two different loading conditions viz., single concentrated load at the

Table 1. Geometrical properties of the girders

Specimens	L (mm)	Panel aspect ratio (b/d)	Slenderness ratio (d/t)	Web, t (mm)	Flanges (top and bottom)		Shear connectors		Reinforced concrete slab
					t_f (mm)	b_f (mm)	t_s (mm)	d_s (mm)	${}^a b_c \times h_c$ (mm)
CPG 1	2400	1.5	250	3	20	200	100	19	1000×150
CPG 2	2400	1.5	150	5	20	260	100	19	1000×150
CPG 7	4800	1.5	250	3	12	160	100	19	1200×150
CPG 8	4800	1.5	150	5	20	235	100	19	1200×150
CPG 1-A	3655	1.5	250	3	20	200	100	19	1000×150

^a b_c denotes effective width of reinforced concrete slab.

mid-span or uniformly distributed load over the entire span were considered in the analyses. Another composite girder, namely CPG 1-A was also introduced and analysed under two symmetrical concentrated loads.

Initially, these analyses were carried out for girders with full interaction with $K = 0.65 \text{ kN/mm}^2$. Additionally, analyses were also carried out on all the girders with four different values of K , obtained by changing the spacing of shear connectors along the span length of the girder. Brief description of the finite element modelling is given in the following section.

5. Finite element analysis

Three-dimensional finite element models were developed using the finite element package, LUSAS for all the girders. Shell and brick elements were used for steel part of the girders and concrete slabs, respectively. Both elements are compatible for non-linear analysis which allows buckling and second-order effects. The steel plate girders were modelled as elastic-perfectly plastic using mild steel material with Poisson's ratio of 0.3. Young's modulus, E_s for S275 steel is taken as 200 GPa while the yield stresses assigned to the flanges, webs and stiffeners vary from 272 MPa to 300 MPa in accordance with those reported in the experiments. The geometrical properties are as per those given in Table 1. Specifically, concrete slab was idealised by hexahedral isoparametric element with six

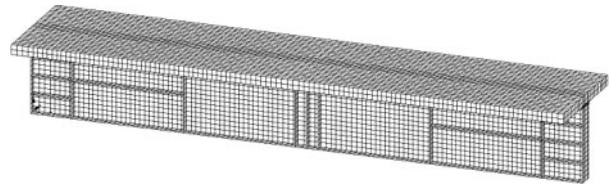


Fig. 5. Typical finite element mesh

degrees of freedom at each node. All material properties assigned for concrete are also based on the experimental data. Strains corresponding to the maximum uniaxial compressive stress and that to the softening end where concrete crushes were adopted as 0.0022 and 0.0035, respectively. Additionally, joint element with specified spring stiffness was assigned at the unmerged steel–concrete interface accordingly to allow for horizontal slide. Total Lagrangian strain formulation along with Crisfield's load incremental procedure was adopted to account for geometric non-linearity in the analysis. Basically, the global stiffness matrix of the structure depends on the displacement increments where the solution of the equilibrium equations is typically accompanied by an iterative method through the convergence check. In the present models, the non-linear Newton–Raphson iterative approach was used by updating the tangent stiffness matrix for each of the iterations (Zubydan, ElSabbagh 2011).

Table 2. Comparison of ultimate loads for girders under single concentrated load at mid-span

Specimens	$K \text{ (kN/mm}^2\text{)}$	$P_u \text{ (kN)}$	$P_{u, \text{ partialint.}} / P_{u, \text{ fullint.}}$	$P_{u, \text{ LUSAS}} \text{ (kN)}$	$P_u / P_{u, \text{ LUSAS}}$
CPG 1	0.65	827	1.0	836	0.99
	0.51	787	0.95	818	0.96
	0.37	746	0.90	793	0.94
	0.31	726	0.88	715	1.02
	0.17	686	0.83	698	0.98
CPG 2	0.65	1355	1.0	1371	0.98
	0.51	1315	0.97	1324	0.99
	0.37	1276	0.94	1282	0.99
	0.31	1255	0.92	1226	1.02
	0.17	1216	0.90	1171	1.04
CPG 7	0.65	754	1.0	760	0.99
	0.51	714	0.94	736	0.97
	0.38	675	0.90	683	0.98
	0.32	653	0.86	625	1.04
	0.19	612	0.81	588	1.04
CPG 8	0.65	1266	1.0	1285	0.98
	0.51	1238	0.98	1281	0.96
	0.38	1210	0.96	1271	0.95
	0.32	1195	0.94	1236	0.96
	0.19	1166	0.92	1134	1.02

A perfectly straight and undeformed model may be stiff and provide different response compared to a model with imperfect geometry. Thus, an imperfection model has been built in LUSAS by loading the results from buckling analysis in which the deformed mesh was considered as initially imperfect geometry of the girders (Basher *et al.* 2011; Chen, Jia 2010). The buckling analysis predicts the possible deformed shapes due to structural instability. The subspace iteration algorithm approximation technique, available in LUSAS facilities, was employed for solving the associated eigenvalue problems. Different deformed shapes were attempted for non-linear analysis. From extensive trials, a mode shape from the first eigenvalue was selected as it provides satisfactory results in terms of ultimate load and behaviour. A typical mesh as shown in

Figure 5 with element size of 50×50 mm was adopted in the analyses. The mesh was chosen based on convergence studies carried out to ascertain the efficiency and effectiveness to provide accurate solutions within an acceptable computational time.

6. Discussion on the results

Results in terms of ultimate loads and load–deflection behaviour were obtained from the proposed method for the girders. The analyses by finite element modelling provided a detailed output from which the ultimate loads and load–deflection plots were extracted. The results for ultimate loads are presented in Tables 2–4 for different load conditions. The ultimate loads obtained by the

Table 3. Comparison of ultimate loads for girders under uniformly distributed load

Specimens	K (kN/mm ²)	w_u (kN/m)	$w_{u, partialint.} / w_{u, fullint.}$	$w_{u, LUSAS}$ (kN/m)	$w_u / w_{u, LUSAS}$
CPG 1	0.65	344	1.0	368	0.93
	0.51	328	0.95	335	0.98
	0.37	311	0.90	299	1.04
	0.31	302	0.88	276	1.09
	0.17	286	0.83	270	1.06
CPG 2	0.65	565	1.0	614	0.92
	0.51	549	0.97	589	0.93
	0.37	532	0.94	578	0.92
	0.31	524	0.93	483	1.08
	0.17	507	0.90	470	1.08
CPG 7	0.65	157	1.0	174	0.90
	0.51	148	0.94	162	0.91
	0.38	140	0.89	150	0.93
	0.32	135	0.86	144	0.94
	0.19	127	0.81	116	1.09
CPG 8	0.65	264	1.0	291	0.91
	0.51	258	0.98	280	0.92
	0.38	252	0.95	269	0.94
	0.32	249	0.94	262	0.95
	0.19	243	0.92	221	1.10

Table 4. Comparison of ultimate loads for girders under two concentrated loads

Specimens	K (kN/mm ²)	P_u (kN)	$P_{u, partialint.} / P_{u, fullint.}$	$P_{u, LUSAS}$ (kN)	$P_u / P_{u, LUSAS}$
CPG 1-A	0.74	409	1.0	430	0.95
	0.60	389	0.95	401	0.97
	0.43	369	0.90	385	0.95
	0.36	359	0.88	370	0.97
	0.21	338	0.83	346	0.97

proposed method are compared with the corresponding finite element values, as shown by the ratios $P_u/P_{u, LUSAS}$ or $w_u/w_{u, LUSAS}$ in the tables, in order to establish the accuracy of the proposed method. Also, ultimate loads for girders with different K values are compared with the corresponding values for the girder with full interaction viz. $K = 0.65 \text{ kN/mm}^2$, as shown by the ratios $P_{u, partialint}/P_{u, fullint}$, so as to assess the influence of

partial interaction on the ultimate strength. Comparison of the ultimate loads shows that the two values are close within the acceptable level of accuracy. In Tables 2–4, the ratio $P_u/P_{u, LUSAS}$ varies from 0.90 to 1.10 indicating that the two values viz. P_u and $P_{u, LUSAS}$ lie within $\pm 10\%$. It is, therefore, confirmed that the proposed method is capable of predicting the shear strength with sufficient accuracy.

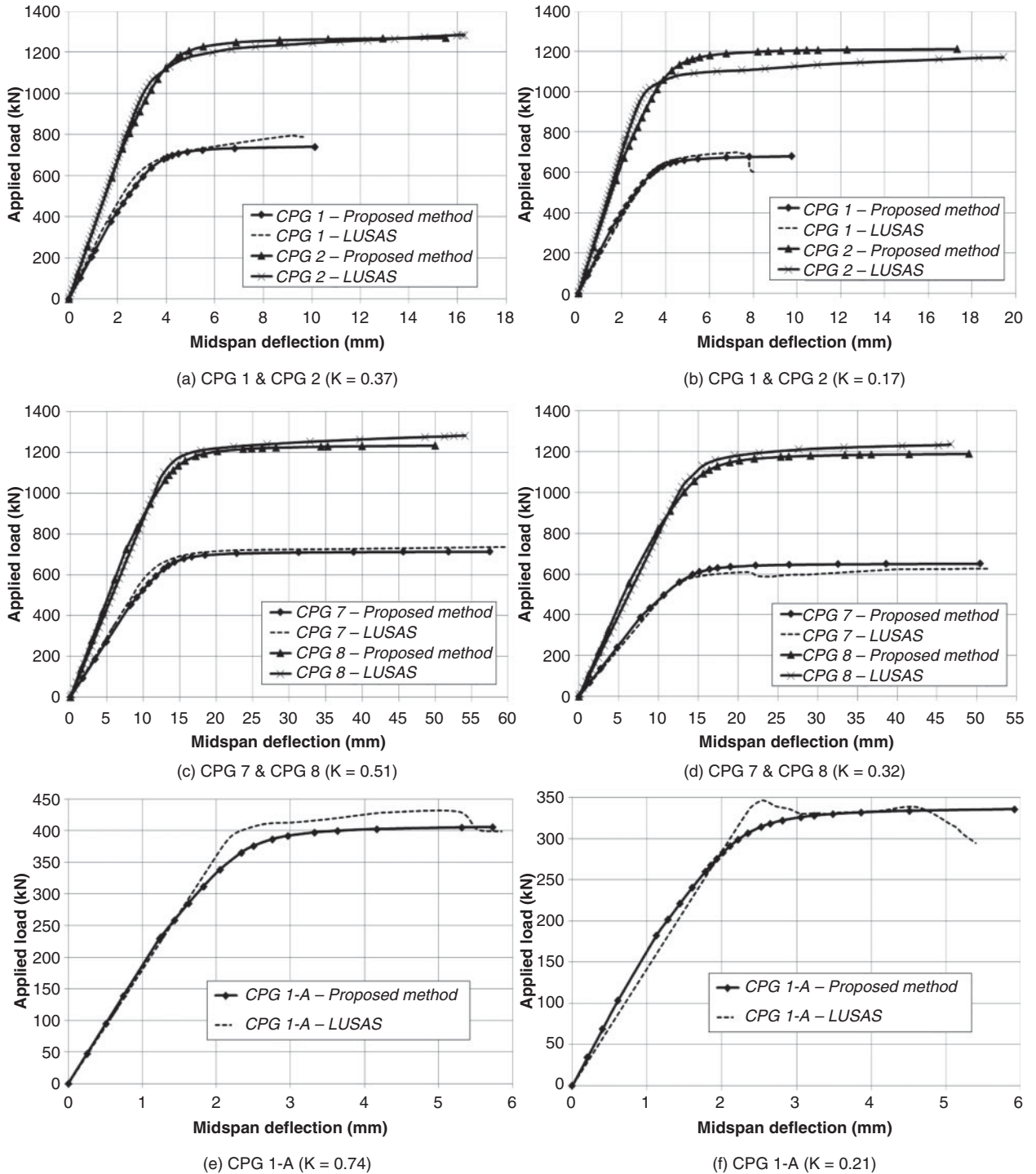


Fig. 6. Comparisons of load-deflection plots – typical behaviour: (a) CPG 1 & CPG 2 ($K = 0.37$); (b) CPG 1 & CPG 2 ($K = 0.17$); (c) CPG 7 & CPG 8 ($K = 0.51$); (d) CPG 7 & CPG 8 ($K = 0.32$); (e) CPG 1-A ($K = 0.74$); (f) CPG 1-A ($K = 0.21$)

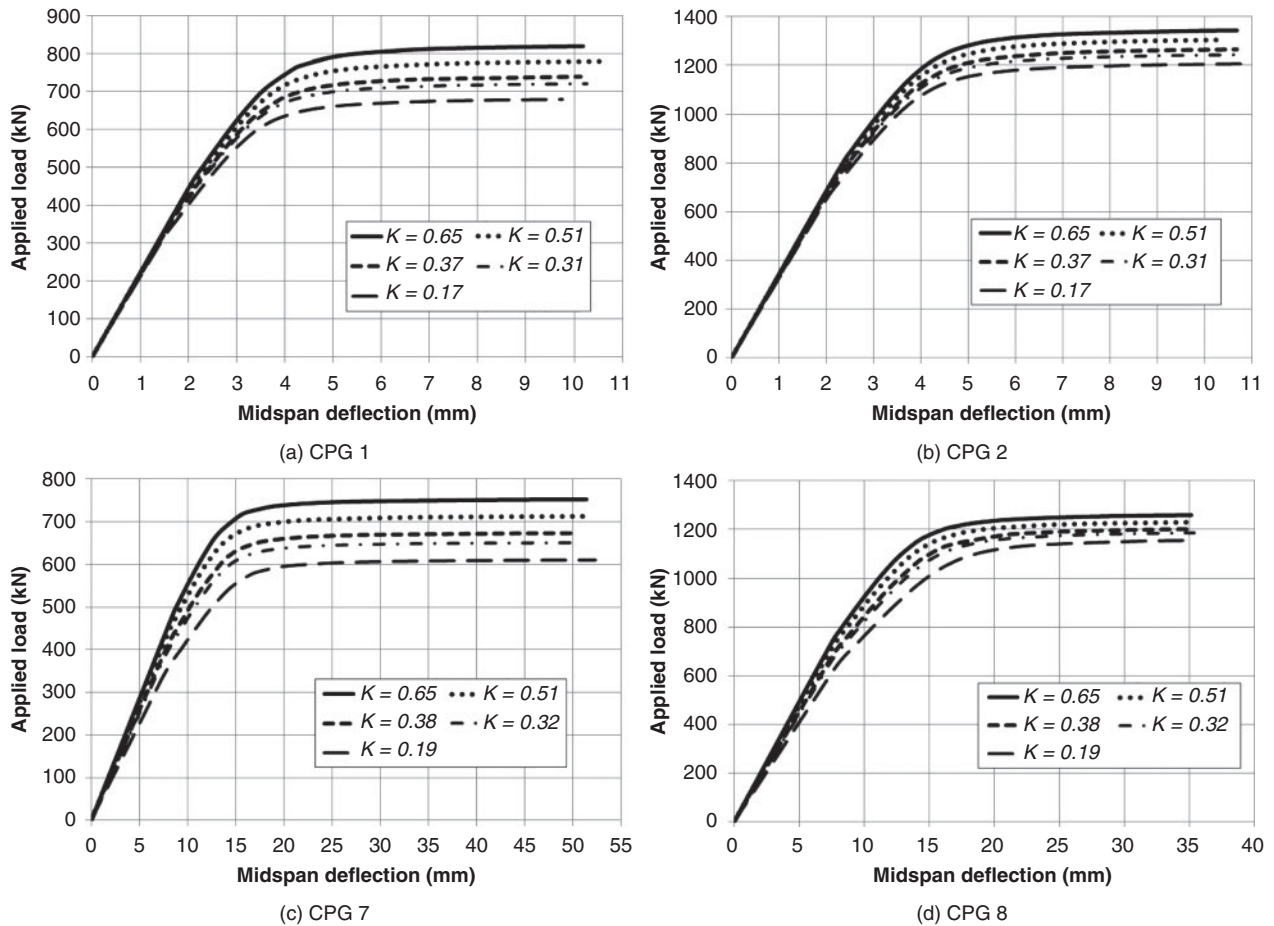


Fig. 7. Behaviour of girders under single concentrated load at mid-span: (a) CPG 1; (b) CPG 2; (c) CPG 7; (d) CPG 8

Comparison of shear strength values for girders with partial interaction with those corresponding to the girders of full interaction is shown in the tables in terms of the ratios $P_{u, partial int.} / P_{u, full int.}$. In Tables 2 and 3, composite girders with $K = 0.65 \text{ kN/mm}^2$ and the one in Table 4 with $K = 0.74 \text{ kN/mm}^2$ are considered as those with full interaction. The remaining girders in which K values are less are considered as those with partial interaction. It is clear from the tables that the ultimate shear strength drops with reduction in degree of interaction. For example, in the girder CPG 1 subjected to a concentrated load shown in Table 2, the girder with $K = 0.17 \text{ kN/mm}^2$, shows 17% drop in the shear strength compared to the one with $K = 0.65 \text{ kN/mm}^2$. This girder under uniformly distributed load also displays same amount of drop in shear strength. The drop is larger viz. 19% in the case of CPG 7 having longer span length. Similar reduction in load carrying capacity can be observed in all the girders with smaller K values. The results presented in the tables also show that the proposed method is capable of predicting the shear strength within the acceptable level of accuracy for all the girders with partial interaction, K value ranging from 0.65 to 0.17 kN/mm^2 . The average value of the ratio $P_u / P_{u, LUSAS}$ in all cases varies from 0.96 to 0.99.

Additionally, the accuracy of the proposed method has also been assessed by comparing the predicted load–

deflection behaviour with the corresponding results obtained from the finite element analyses. Typical results presented in Figure 6 show the variation of mid-span deflection with the applied load for selected girders with different K values. It can be seen from the figures that the two results are very close to each other from the initial stage of loading to the ultimate load condition. The observation is true for different loading conditions and for different K values. The results show that the proposed method is also capable of predicting the behaviour with sufficient accuracy.

The flexural behaviour of the girders obtained by the proposed method is also illustrated in Figures 7–9, in which load–deflection plots are shown for girders subjected to single concentrated load applied at the mid-span, uniformly distributed load and two point loads, respectively. In each of the figures, load–deflection curves for girders having different values of K are presented in order to show the extent of influence of this parameter on the behaviour of the girders. It is clear from the figures that ultimate load drops with different rate and magnitude of drop as the value of K is reduced from full degree of interaction to negligible amount of interaction. Stiffness of the girders at the initial stages of loading is marginally affected with the variation in the K values. This

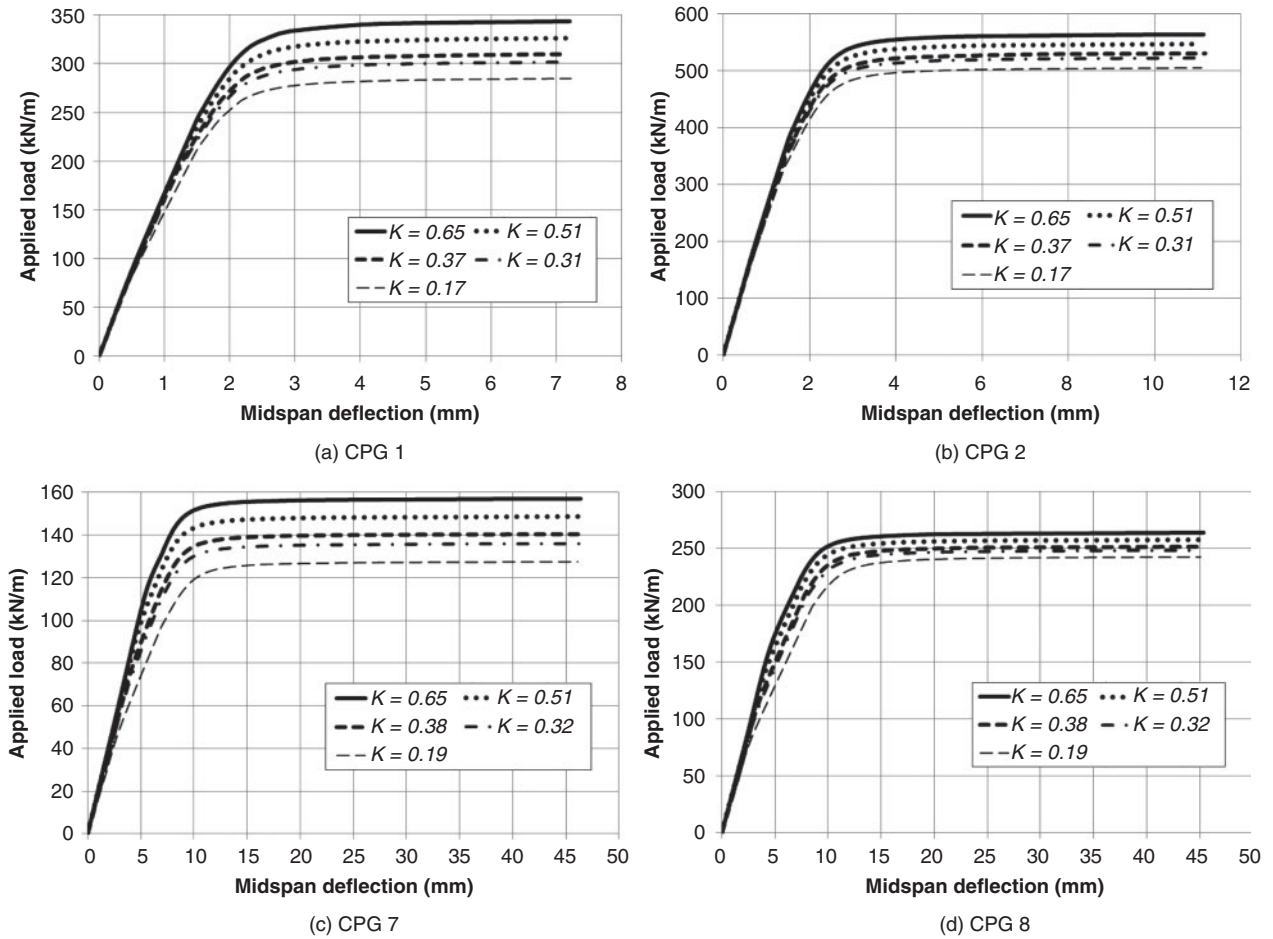


Fig. 8. Behaviour of girders under uniformly distributed load: (a) CPG 1; (b) CPG 2; (c) CPG 7; (d) CPG 8

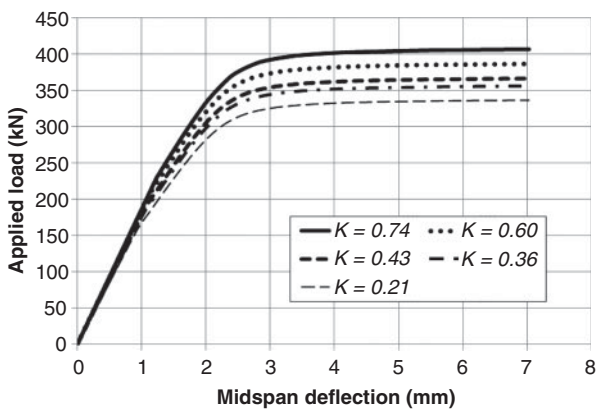


Fig. 9. Behaviour of girder CPG 1-A subjected to two concentrated loads

observation is true irrespective of the girders and the loading patterns.

Conclusions

An approximate method to determine the behaviour and flexural capacity of composite plate girders with partial shear connection is presented in this paper. The girders considered include those subjected to concentrated or uniformly distributed loads. The accuracy of the method

has been established by comparing the results with the corresponding results obtained by finite element method using LUSAS software. Additionally, effect of varying the degree of interaction has been examined by analysing the girders with different degrees of interaction. It is found from the results presented herein that the proposed method is accurate enough to predict the behaviour of composite plate girders under different types of loading and that the method could account for variation in degree of interaction. It is observed that the bending stiffness and load carrying capacities of the girders reduced with decreasing degree of interaction. The drop in ultimate load with degree of interaction varies with the loading type, significant in some cases and negligible in certain cases.

Acknowledgement

The authors acknowledge the support provided by the Department of Civil and Structural Engineering, Universiti Kebangsaan, Malaysia.

References

Adekola, A. O. 1968. Partial interaction between elastically connected elements of a composite beam, *International Journal of Solids and Structures* 4: 1125–1135. [http://dx.doi.org/10.1016/0020-7683\(68\)90027-9](http://dx.doi.org/10.1016/0020-7683(68)90027-9)

- Allison, R. W.; Johnson, R. P.; May, I. M. 1982. Tension field action in composite plate girders, *Proceedings of the Institution of Civil Engineers*, London, 73: 255–276.
- Basher, M.; Shanmugam, N. E.; Khalim, A. R. 2011. Horizontally curved composite plate girders with trapezoidally corrugated webs, *Journal of Constructional Steel Research* 67: 947–956. <http://dx.doi.org/10.1016/j.jcsr.2011.01.015>
- Baskar, K.; Shanmugam, N. E. 2003. Steel–concrete composite plate girders subject to combined shear and bending, *Journal of Constructional Steel Research* 59: 531–557. [http://dx.doi.org/10.1016/S0143-974X\(02\)00042-1](http://dx.doi.org/10.1016/S0143-974X(02)00042-1)
- Baskar, K.; Shanmugam, N. E.; Thevendran, V. 2002. Finite element analysis of steel–concrete composite plate girder, *Journal of Structural Engineering* 128: 1158–1168. [http://dx.doi.org/10.1061/\(ASCE\)0733-9445\(2002\)128:9\(1158\)](http://dx.doi.org/10.1061/(ASCE)0733-9445(2002)128:9(1158))
- Bradford, M. A.; Gilbert, R. I. 1992. Composite beams with partial interaction under sustained loads, *Journal of Structural Engineering* 118(7): 1871–1883. [http://dx.doi.org/10.1061/\(ASCE\)0733-9445\(1992\)118:7\(1871\)](http://dx.doi.org/10.1061/(ASCE)0733-9445(1992)118:7(1871))
- Chen, S.; Jia, Y. 2010. Numerical investigation of inelastic buckling of steel–concrete composite beams prestressed with external tendons, *Thin-Walled Structures* 48: 233–242. <http://dx.doi.org/10.1016/j.tws.2009.10.009>
- Eurocode 2. 2004. *Design of concrete structures*. British Standards Institution. Brussels.
- Evans, H. R.; Porter, D. M.; Rockey, K. C. 1978. The collapse behaviour of plate girders subjected to shear and bending, in *Proc. of the International Association for Bridge and Structural Engineering (IABSE) Colloquium*, Bergamo, vol. 4: 1–20.
- Girhammar, U. A. 2009. A simplified analysis method for composite beams with interlayer slip, *International Journal of Mechanical Sciences* 51: 515–530. <http://dx.doi.org/10.1016/j.ijmecsci.2009.06.004>
- Johnson, R. P. 2004. *Composite structures of steel and concrete*. 3rd ed. Oxford: Blackwell Scientific Publications. Oxford. <http://dx.doi.org/10.1002/9780470774625>
- Liang, Q. Q.; Uy, B.; Bradford, M. A.; Ronagh, H. R. 2004. Ultimate strength of continuous composite beams in combined bending and shear, *Journal of Constructional Steel Research* 60: 1109–1128. <http://dx.doi.org/10.1016/j.jcsr.2003.12.001>
- Narayanan, R.; Al-Amery, R. I. M.; Roberts, T. M. 1989. Shear strength of composite plate girders with rectangular web cut-outs, *Journal of Constructional Steel Research* 12: 151–166. [http://dx.doi.org/10.1016/0143-974X\(89\)90030-8](http://dx.doi.org/10.1016/0143-974X(89)90030-8)
- Newmark, N. M.; Siess, C. P.; Viest, I. M. 1951. Test and analysis of composite beams with incomplete interaction, in *Proceedings of the Society for Experimental Stress Analysis*, 9(1): 75–92.
- Nie, J.; Cai, C. S. 2003. Steel–concrete composite beams considering shear slip effects, *Journal of Structural Engineering* 129: 495–506. [http://dx.doi.org/10.1061/\(ASCE\)0733-9445\(2003\)129:4\(495\)](http://dx.doi.org/10.1061/(ASCE)0733-9445(2003)129:4(495))
- Oehlers, D. J.; Nguyen, N. T.; Ahmed, M.; Bradford, M. A. 1997. Partial interaction in composite steel and concrete beams with full shear connection, *Journal of Constructional Steel Research* 41: 235–248. [http://dx.doi.org/10.1016/S0143-974X\(97\)80892-9](http://dx.doi.org/10.1016/S0143-974X(97)80892-9)
- Porter, D. M.; Cherif, Z. E. A. 1987. Ultimate shear strength of thin webbed steel and concrete composite girders, in *Proc. of the International Conference of Steel and Aluminium Structures*, London, 55–64.
- Porter, D. M.; Rockey, K. C.; Evans, H. R. 1975. The collapse behaviour of plate girders loaded in shear, *The Structural Engineer* 53: 313–325.
- Queiroz, F. D.; Vellasco, P. C. G. S.; Nethercot, D. A. 2007. Finite element modelling of composite beams with full and partial shear connection, *Journal of Constructional Steel Research* 63: 505–521. <http://dx.doi.org/10.1016/j.jcsr.2006.06.003>
- Seracino, R.; Lee, C. T.; Lim, T. C.; Lim, J. Y. 2004. Partial interaction stresses in continuous composite beams under serviceability loads, *Journal of Constructional Steel Research* 60: 1525–1543. <http://dx.doi.org/10.1016/j.jcsr.2004.01.002>
- Seracino, R.; Lee, C. T.; Tan, Z. 2006. Partial interaction shear flow forces in continuous composite steel–concrete beams, *Journal of Structural Engineering* 132(2): 227–236. [http://dx.doi.org/10.1061/\(ASCE\)0733-9445\(2006\)132:2\(227\)](http://dx.doi.org/10.1061/(ASCE)0733-9445(2006)132:2(227))
- Shanmugam, N. E.; Baskar, K. 2003. Steel–concrete composite plate girders subject to shear loading, *Journal of Structural Engineering* 129: 1230–1242. [http://dx.doi.org/10.1061/\(ASCE\)0733-9445\(2003\)129:9\(1230\)](http://dx.doi.org/10.1061/(ASCE)0733-9445(2003)129:9(1230))
- Timoshenko, S. P.; Gere, J. M. 1961. *Theory of elastic stability*. 2nd ed. New York: McGraw-Hill Book Company.
- Uy, B.; Nethercot, D. A. 2005. Effects of partial shear connection on the required and available rotations of semi-continuous composite beam systems, *The Structural Engineer* 83(4): 29–39.
- Xu, R.; Wu, Y. F. 2007. Two-dimensional analytical solutions of simply supported composite beams with interlayer slips, *International Journal of Solids and Structures* 44: 165–175. <http://dx.doi.org/10.1016/j.ijsolstr.2006.04.027>
- Zubydan, A. H.; ElSabbagh, A. I. 2011. Monotonic and cyclic behavior of concrete-filled steel-tube beam-columns considering local buckling effect, *Thin-Walled Structures* 49: 465–481. <http://dx.doi.org/10.1016/j.tws.2010.12.007>

Md Y. YATIM. A PhD candidate at the Department of Civil and Structural Engineering, Kebangsaan University, Malaysia. His research interests include steel–concrete composite structures, computational mechanics, structural concrete and steel, high-rise structures, etc.

Nandivaram E. SHANMUGAM. A Professor at the Department of Civil and Structural Engineering, Kebangsaan University, Malaysia. He obtained his PhD degree from the University of Wales (Cardiff) in 1978. He has taught at undergraduate and graduate levels for more than 45 years. He has published more than 200 scientific papers in international journals and conference proceedings. He is a member of the editorial board of *Journal of Constructional Steel Research*, *Thin-Walled Structures*, *Journal of Structural Stability and Dynamics*, *International Journal of Steel Composite Structures*, *International Journal of Steel Structures* and *IES Journal Part A: Civil and Structural Engineering*. He is a Chartered Engineer (CEng), Fellow of the Institution of Structural Engineers, London, (FIStructE), Fellow of the Royal Institution of

Naval Architects (FRINA), Fellow of the American Society of Civil Engineers (FASCE), Fellow of the Institution of Engineers, Singapore (FIES) and Fellow of the Institution of Engineers, India (FIEI). His research interests include steel plated structures, steel–concrete composite construction, long-span structures and connections, cold-formed steel structures, elastic and ultimate load behaviour of steel structures, etc.

Wan BADARUZZAMAN. A Professor at the Department of Civil and Structural Engineering, Kebangsaan University, Malaysia. He received his PhD degree from the University of Wales (Cardiff) in 1994 and has taught at undergraduate and graduate levels for more than 25 years. He is the author and the co-author of many scientific papers in international journals and conference proceedings. He is a corporate member of the Institution of Engineers, Malaysia (MIEM). His research interests include behaviour of lightweight composite structures, industrialised building system, reinforced concrete design and construction, computational analysis, etc.